

**Feasibility Study And Design Concept For An Orbiting Ice-Penetrating
Radar Sounder To Characterize In Three-Dimensions The European Ice
Mantle Down To (And Including) Any Ice/Ocean Interface.**

25 June, 1999

Prepared by the Europa Radar Sounder Instrument Definition Team:

D. D. Blankenship, Chair, University of Texas at Austin
B. C. Edwards, Co-Chair, Los Alamos National Laboratory
Y. Kim, Co-Chair, Jet Propulsion Laboratory
P. E. Geissler, University of Arizona
D. Gurnett, University of Iowa
W. T. K. Johnson, Jet Propulsion Laboratory
W. Kofman, Observatoire de Grenoble, France
J. C. Moore, University of Lapland
D. L. Morse, University of Texas at Austin
R. T. Pappalardo, Brown University
G. Picardi, University of Rome, Italy
R. K. Raney, Johns Hopkins University
E. R. Rodriguez, Jet Propulsion Laboratory
X.-M. Shao, Los Alamos National Laboratory
J. Weertman, Northwestern University
H. A. Zebker, Stanford University
J. van Zyl, Jet Propulsion Laboratory

Some of the research described in this publication was carried out at the Jet Propulsion Laboratory, California Institute of Technology, under a contract with the National Aeronautics and Space Administration.

Table of Contents

Table of Contents	i
1. Philosophy of the Europa Radar Sounder	1
2. Sounding Model	2
<i>Absorption.....</i>	<i>4</i>
<i>Scattering</i>	<i>8</i>
<i>System Performance.....</i>	<i>11</i>
3. Hardware.....	13
<i>Antenna Characteristics.....</i>	<i>14</i>
<i>Signal Generator.....</i>	<i>15</i>
<i>Transmitter.....</i>	<i>16</i>
<i>Receiver.....</i>	<i>15</i>
<i>Digital Electronics</i>	<i>16</i>
<i>System Parameters</i>	<i>16</i>
<i>Mass/Power Estimate.....</i>	<i>17</i>
<i>Spacecraft Interface Assumptions</i>	<i>18</i>
4. Processing	18
<i>On-board Processing</i>	<i>19</i>
<i>Requirements.....</i>	<i>20</i>
<i>Constraints</i>	<i>20</i>
<i>Mode descriptions</i>	<i>21</i>
Mode 1: Full-Resolution Waveforms (FW).....	22
Mode 2: Averaged Waveforms (AW).	22
Mode 3: Radar Sounder Data Record (RDR).....	23
5. Sampling Strategy	23
6. Other Applications of the Radar Sounder	24
References.....	25

1. Philosophy of the Europa Radar Sounder

A primary objective of the Europa Orbiter Mission is the detection of any ocean that may lie beneath Europa's icy shell. Another primary objective is to characterize the distribution of the subsurface water associated with any ocean as well as the overlying ice. This will require either direct or inferred knowledge of the position (in three dimensions) of any ice/water interface. It is well known from studies of Earth's ice sheets that radar sounding at frequencies of tens to a few hundred MHz can be used to sound ice bodies that are many kilometers in thickness. Similarly, airborne radar sounding has proven to be a powerful tool for detecting and characterizing water bodies (both lakes and ocean) beneath these ice sheets. However, the question remains whether these techniques are appropriate for probing Europa's icy shell. The intent of this document is to address these uncertainties.

The Science Definition Team for the Europa orbiter has recommended globally distributed radar sounding with a "depth resolution of 100 m at the surface decreasing with depth, spatial resolution at or better than the scale of major surface features, and designed to maximize the likelihood of detection of an ice/liquid interface". The thickness of ice that can be sounded on Europa is determined by the absorption of electromagnetic waves in the ice (which is dictated by its temperature and impurity content) and scattering characteristics of the ice body (including the surface and basal interfaces as well as any volume scatterers). Because of the variety of surface terrain types observed on Europa and geologic processes inferred to be at work, we expect Europa's absorption and scattering properties to be spatially inhomogeneous and its crustal ice thickness to be locally variable. The scattering properties of any assumed sounding model for Europa, as well as the Jovian radio noise environment (Figure 1), are frequency-dependent. Earth-based radar sounding of Europa at 3.5- and 13-cm wavelengths suggests that Europa's ice crust contains many high-order multiple scattering inhomogeneities in its uppermost few meters at decimeter scales, which prohibits probing of the ice to any great depth at these wavelengths. However, sounding at 70-cm indicates that scattering inhomogeneities at that wavelength are far fewer. Therefore, radar sounding appears viable at wavelengths of a few meters.

We present below a sounding model (Section 2) based on the range of current working hypotheses for the nature of Europa's icy shell. Based on Jovian noise considerations and the sounding model, the Instrument Definition Team for the Europa Radar Sounder has converged on the selection of 50 MHz as the sounding frequency (implemented using a multi-element array). The recommended radar sounder hardware (Section 3) is coupled to an on-board processing design (Section 4) and sampling strategy (Section 5) intended to optimize the ability of the Europa Orbiter to characterize in three dimensions the global distribution of any ice/water interface either directly, or inferred from other significant geophysical interfaces. It is the Instrument Definition Team's belief that, even under the worst case assumptions, any extensive liquid that lies within a few kilometers of the surface (i.e., conceivably within reach of future spacecraft exploration) will be detected by the radar instrument described in this document. Moreover, through sounding the shallow subsurface of the satellite and characterizing any geologically significant interfaces encountered, we expect considerable advances in our understanding of Europa even in those areas where any ice/water interface may not be directly observable.

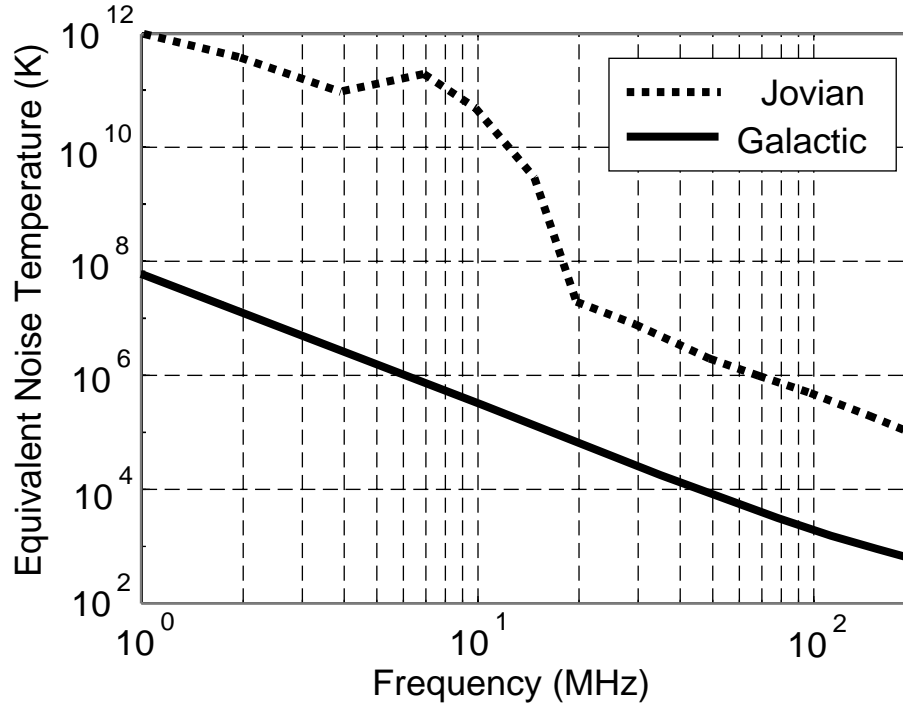


Figure 1. The Europa radio frequency noise environment (S. Gulkis, personal communication).

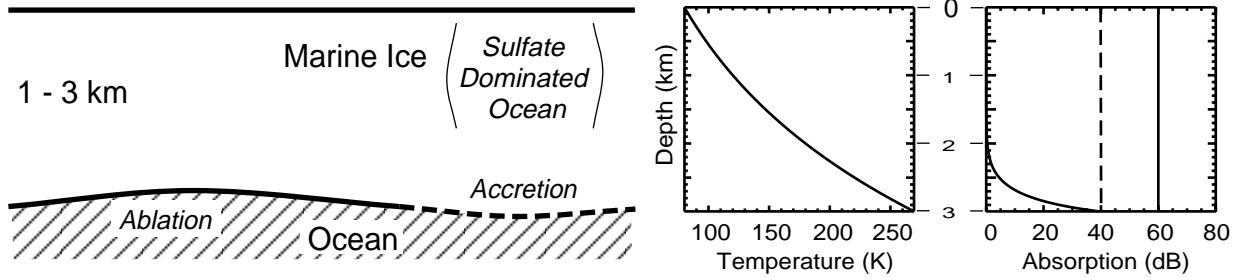
2. Sounding Model

On Earth, naturally occurring ice can be classified into three basic types: atmospheric precipitation that forms the glaciers and ice sheets is known as *meteoric ice*; ice that accretes beneath the large ice shelves of Antarctica from frazil ice crystals which form directly in the ocean water, is called *marine ice*; and ice formed by freezing of water close to the atmospheric interface as typified by *sea ice*. Meteoric ice cannot be present on Europa in any quantities because of the lack of a significant atmosphere. However, there is a good chance that ice formation processes at an ice/ocean interface on Europa would be similar to those on Earth, suggesting that marine ice and sea ice analogs are relevant.

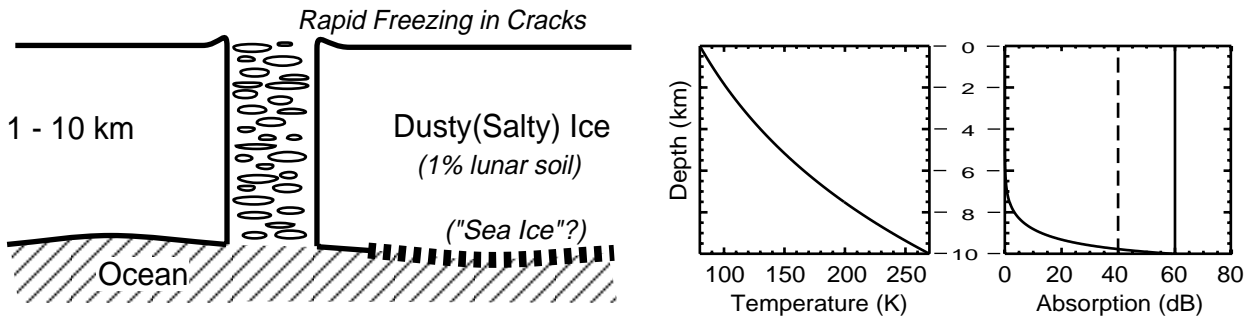
We consider three models to represent ice growth mechanisms that may be present on Europa. First, a marine-ice European crust (Fig. 2A) with slow accretion (freezing) or ablation (melting) on the lower side of the icy crust with temperature gradients that are primarily a function of ice thickness. A second possible mechanism is the very rapid freezing of ocean water in the linear fracture zones caused by tidal/tectonic processes where large temperature gradients will be present. This process could lead to ice with properties similar to sea ice although water reaching the surface could be very unlike sea ice because of very rapid boiling. This “tidal/tectonic” model (Figure 2B) could represent an oceanic imprint on a primordial European crust that had been well below the melting point throughout its history, or could represent the ice formed entirely by ocean water injected in cracks and then spread over much of the crust by tidally

Figure 2 (caption). Schematic diagrams of three ice formation processes that may occur on Europa with expected temperature and radar absorption versus depth for each assuming a “mid-latitude” surface temperature of 80 K. The range of ice thickness (which is highly uncertain) for the models is taken from Pappalardo et al. (submitted) and the properties of the component ices and ocean are given in Table 1. *A* is a model of ice formation similar to that for marine ice on Earth (e.g., Europa’s chaotic terrains) with parts of the base subject to melting (ablation) and others to slow freezing (accretion) of frazil ice crystals; *B* indicates ice formation via extrusion into cracks or fissures with rapid freezing (e.g., Europa’s ridged plains); *C* gives a convection scenario with a cold rigid crust underlain by thicker isothermal convecting ice. The dashed vertical line on the absorption versus depth plots for these models indicates the approximate dynamic range of the proposed radar sounder (Figure 3) given the levels of sub-Jovian radio frequency noise at 50 MHz (Figure 1); the dynamic range corresponding to the galactic background noise (Figure 1) expected to limit radar sounding on anti-Jovian Europa is given by the solid vertical line. Note that for both the “marine ice” (*A*) and “tidal/tectonic” (*B*) examples, a reasonably smooth ice/ocean interface with properties derived from the non-sea-ice entries of Table 1 (i.e., a reflection coefficient of about -3db) can be well characterized. In addition, the reduced reflection strength from dusty-ice (salty-ice) / sea-ice interfaces (e.g., a reflection coefficient of about -20dB) should still allow the base of the rigid crust for the convection model (*C*) to be detected and characterized. A final important result is that the negligible absorption for the upper 80% of the non-isothermal conducting ice for all three models could allow even very weakly reflecting geophysical interfaces to be imaged

A) Marine Ice Processes



B) Tidal/Tectonic Processes



C) Convection Processes

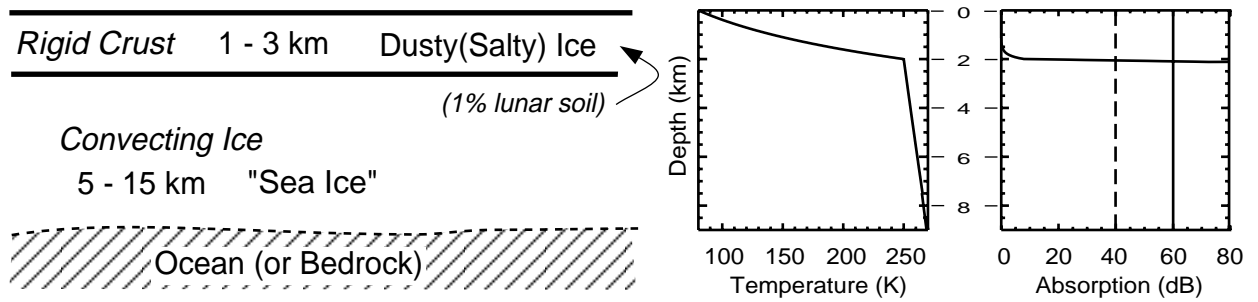


Figure 2.

driven tectonic processes. In addition to these two processes, Pappalardo et al. (1998) use evidence from Galileo imagery to support the idea of convection in an isothermal layer under a rigid ice crust up to a few km thick that is thermally conducting (Figure 2C). This convecting ice model could be dominated by ice very similar to that for the tidal/tectonic model although subject to a dramatically different thermal regime..

Absorption

The absorption of radar waves in ice formed by the processes outlined in Figure 2 is dependent on the ice temperature as well as the nature and concentration of any impurities. Experiments on ice grown in laboratories and on naturally occurring ices have shown that soluble impurities can be incorporated into the ice lattice where they generate electrical defects (Gross et al., 1977, 1978; Glen and Paren, 1975; Moore et al., 1992, 1994). At radar sounding frequencies of 10's to 100's of MHz, the absorption rate of electromagnetic waves (α) in ice can be written as:

$$\alpha \approx 0.0009 \sigma \text{ dB m}^{-1}$$

where σ is the electrical conductivity (in $\mu\text{S m}^{-1}$). Comparison of electrical conductivity measurements on meteoric and laboratory ice at relatively low frequency (about 100 kHz) with data from much higher radar and microwave frequencies suggests that there are no significant dielectric dispersions in the radar sounding range even with varying concentration of soluble impurities (Glen and Paren, 1975; Moore and Fujita 1993).

Corr et al. (1993) show that the electrical conductivity for ice can be expressed as a series of Arrhenius functions with impurity specific activation energies and constants:

$$\sigma = \sum_{i=1}^3 C_i \exp \left[\frac{-E_i}{k} \left(\frac{1}{T} - \frac{1}{T_r} \right) \right]$$

where T is absolute temperature, T_r is a reference temperature of 251 K and k is the Boltzmann constant. C_i represents the conduction contribution from the various components in the ice: an intrinsic pure ice term amounting to $4.5 \mu\text{S m}^{-1}$, and acid (H^+) and chloride terms with molar conductivities of 4 S m^{-1} and 0.5 S m^{-1} at T_r , respectively (Moore and Fujita, 1993). E_i is the species specific activation energy which for pure ice is rather high, about 0.6 eV (58 kJ/mol, Glen and Paren, 1975), compared with those for impurities (Corr et al., 1993). This means that the relative importance of the pure ice term rapidly diminishes with decreasing temperature, while the effects of soluble impurities dominate.

The species of impurity that are known to have non-negligible solubility in ice are the NH_4^+ , H^+ , F^- , and Cl^- , (Gross et al., 1978). It is likely that ammonium salts play no part in European ice formation as temperatures in the nebula where Europa formed probably exceeded the condensation temperature for ammonium hydrate (Kargel, 1991). If large amounts of sulfate exist in any ocean on Europa it is possible that some H_2SO_4 may be present which could

contribute H^+ to the ice; however, these acids would be neutralized by any carbonates in a European ocean. Carbonates, which are commonly seen in leachates from meteorites (Fanale et al., 1977) and are consistent with spectroscopy observations of surface salts on Europa (McCord et al., 1998), are likely to be present in any European Ocean. Because F^- is cosmogenically rather rare, we are left with Cl^- as the dominant soluble impurity in ice. The activation energy for Cl^- from marine and meteoric ice on Earth over a wide range of concentrations and at temperatures down to 210 K is 0.19 eV, (18.4 kJ/mol, Moore et al., 1992).

For impurity concentrations in the ice above a species dependent solubility limit, the species must be present outside the crystal structure as a liquid or separate salt phase. Additional radar losses can come from interfacial polarizations and scattering that occurs whenever the radar waves encounter these mixtures of insoluble impurities. Examples of these mixtures would be dusty or salty ice or, in the extreme case, sea ice where mm-scale brine pockets are trapped in the ice by rapid freezing. Because of the large difference in dielectric constant between liquid brine and ice (typical dielectric constants of 86 and 3.2, respectively; Moore et al., 1992), sea ice is characterized by very large absorption at radar frequencies.

Table 1 presents the absorption at radar sounding frequencies for a range of ices consistent with the European ice formation processes presented in Figure 2. End members of the table are pure ice with the conductivity and activation energy given by Glen and Paren (1975) and sea ice formed in the relatively low salinity (3 parts per thousand; ppt) Bay of Bothnia in the Baltic Sea where ice salinities are about 0.5–1ppt and brine pockets are common (Weeks et al., 1990).

Our preferred model for marine ice formation is based on a straightforward model of the geochemical evolution of Europa (Kargel 1991) which predicts the icy crust to be largely dominated by sulfate salts, mainly $MgSO_4$ and Na_2SO_4 ; however, there could also be about 1% by weight Cl^- , mainly as $NaCl$ and $MgCl_2$. All these salts are highly soluble in water and any ocean with the composition predicted by models similar to Kargel (1991) will be hypersaline in sulfate salts. This is in agreement with leachates obtained from carbonaceous chondrites, thought to be representative of the original composition of Europa (Fanale et al., 1977; 1998). The calculation of absorption for the marine ice models requires an estimate of the distribution coefficient, k , for the Cl^- concentration in ice relative to that in the liquid it is grown in. Table 1 uses a distribution coefficient for marine ice, $k_{MI} = 7 \times 10^{-4}$ (Moore et al., 1994), that is derived from measurements on samples that formed under accretion rates observed for the Ronne Ice Shelf. As an unlikely end member for marine-ice processes we have calculated the absorption losses for the marine ice of Antarctica's Ronne Ice Shelf using experimental values of conductivity that are well known over the temperature range 0° to $-70^\circ C$ (Moore et al., 1994). For marine ice formed by a "chloride dominated" European ocean, we have used a direct comparison of the ocean volume to crust ratio for Europa and Earth. A thickness of 100 km for the ice/water crust of Europa corresponds to a volume that is similar to that of Earth's ocean. Given that the land surface of Earth is about 10 times that of Europa, a simplistic estimate for European ocean chlorinity is about $1/10$ that of Earth's oceans or about 3.5 ppt. However, considering the lack of granitoid continental crust and the improbability of rates of European weathering similar to those on the early Earth, this is likely to be a significant overestimate.

For our preferred “sulfate-dominated” Europa Ocean, it is important to note that sulfate ions are not soluble in ice to any significant degree and experiments on ice formed naturally on Earth (and in laboratories) show that SO_4^{2-} seems to play no role in electrical conduction (Gross et al., 1978). Because the permittivity of these solid salts would be similar to that for rock, the tidal/tectonic processes of Figure 2 assume “dusty (salty) ice” derived from Chyba et al. (1998) who modeled the icy crust of Europa as 1%, 10%, and 50% lunar soil mixed with pure ice, and no soluble impurities. These mixtures of rock (or salt) contribute to absorption through the differences in permittivity between pure ice and the rock components using a Rayleigh mixing formula for spherical scattering bodies in a background medium. We believe that Chyba’s 1% soil mixture is an acceptable representation of the absorption of a “sulphate dominated” icy crust on Europa that is being generated/modified by either tidal/tectonic or convection processes.

Given the ice formation processes of Figure 2, Table 1 presents the calculated radar absorption averaged over the total ice thickness for a range of possible European ice; in addition, Figure 2 presents the calculated temperature and absorption as a function of depth ($T(z)$ and $\alpha(z)$, respectively) for these ice formation processes. The strong temperature dependence of electrical conductivity in ice dictates that the temperature profile in the European ice layer is a major factor in total radar absorption. Chyba et al., (1998) pay particular attention to the temperature profile for the thermal conducting layer cases (i.e., “marine” ice and tidal/tectonic processes as well as the rigid shell of the convection processes). For a simple conducting ice layer

$$T(z) = T_s \exp(z/b)$$

where the surface temperature is T_s at $z = 0$ and $b = h / \ln(T_b/T_s)$ where h is the ice thickness and T_b is the temperature at the ice base; the surface temperatures on Europa range from about 100K at the equator to 50K at the poles. For the marine-ice and tidal/tectonic processes of Figure 2, T_b will be close to 270K for reasonable ice thicknesses. In the case of convecting processes, where a cold brittle outer crust is underlain by warmer convecting ice that is nearly isothermal at perhaps 235°-260°K (Pappalardo et al., 1998; Chyba et al., 1998; McKinnon, in press), the value of T_b for the conducting layer can be taken to be the temperature of the isothermal layer. Since the radar absorption is governed by the exponential dependence on temperatures, an average two-way absorption (per km) that is independent of total ice thickness can be found for a given surface temperature. Table 1 gives the averaged two-way radar absorption per km of total ice thickness for two conducting models: one with $T_b=270\text{K}$ corresponding to marine-ice or tidal/tectonic processes and one with $T_b = 250\text{K}$ corresponding to the cold brittle shell of the “convection” process. The range of absorption for each of the conducting models in Table 1 corresponds to the range of surface temperatures (50-100K) on Europa.

Europa Radar Sounder Instrument Definition

Table 1: Radar absorption for various ice types and temperatures. Absorption, α , is in dB/m at 251 K. Columns I and II are computed two-way averaged absorption over the total ice thickness, in dB/km, for ice shells with base temperatures of 270 and 250 K, respectively; these values are independent of shell thickness since the temperature profile is stretched to the ice thickness. The range of values for each Column I or II entry corresponds to surface temperatures of 50 and 100 K. Lighter row shading illustrates our assumptions regarding increasingly likely electrical properties for Europa's ice crust. The distribution coefficient affecting the marine ice models comes from Ronne Ice Shelf marine ice measurements. Note that the absorption losses for the dusty (salty) ice models are calculated using pure-ice behavior consistent with the existing Table 1 entry which leads to small differences from the losses given in Chyba et al., (1998).

Ice Type	Impurity Content	α (dB m ⁻¹)	I (dB km ⁻¹)	II (dB km ⁻¹)	Notes
Pure Ice	Nil	0.0045	1.4 - 2.4	0.2 – 0.3	Glen and Paren (1975)
Marine Ice (Chloride dominated Europa ocean)	3.5 ppt chlorinity ocean	0.016	4 - 7	1.6 – 2.8	Scaled from Earth ocean, $k_{MI} = 7 \times 10^{-4}$
Dusty (Salty) Ice	1% lunar soil (or salt)	0.008	5 – 6	3.6 – 4.1	Chyba et al., (1998) recalculated
Dusty (Salty) Ice	10% lunar soil (or salt)	0.01	8 – 9	6 – 7	Chyba et al., (1998) recalculated
Marine Ice (Sulfate dominated Europa ocean)	10 ppt chlorinity ocean	0.037	9 - 16	4 – 7	Kargel, (1991); $k_{MI} = 7 \times 10^{-4}$
Dusty (Salty) Ice	50% lunar soil (or salt)	0.021	30 - 33	28 – 31	Chyba et al., (1998) recalculated
Marine Ice (Ronne Ice Shelf)	0.025 ppt chlorinity ice(\approx 35 ppt chlorinity ocean)	0.15	36 - 61	18 - 31	Moore et al.,(1994)
Sea Ice (Baltic Sea)	\approx 3 ppt chlorinity ocean	0.85 (at 270K)	50 - 85	16 - 27	200 MHz radar measurement

Scattering

Observed from Earth, the radar return from Europa's surface decreases significantly as the wavelength increases (Ostro et al., 1992; Ostro, private comm., 1998); this suggests that low-frequency returns from Europa may be due to scattering mechanisms similar to those operating from Earth's icy surfaces. Standard scattering theories require knowledge of the ice dielectric constant and the surface height spectrum (Tsang et al., 1985). As shown above, the imaginary part of the dielectric constant (which is proportional to the electrical conductivity) is a strong function of both temperature and salinity; however, the Fresnel reflection coefficient is dominated by the real part, which is nearly insensitive to these parameters. The results below assume a Fresnel reflection coefficient similar to that observed for Earth's icy surfaces.

A two-scale scattering model (Tsang, 1985), has been used successfully to characterize radar returns from a variety of rough surfaces on Earth. This model predicts that the total radar cross section will be the sum of two contributions: Bragg scattering interactions due to surface spectral components whose scale is smaller than some critical wavelength (the so-called spectral cutoff) and geometrical optics contributions due to large scale components with wavelengths greater than the spectral cutoff. The large scale components tilt the small scale patches to produce specular returns when the tilt is aligned appropriately (relative to the transmitting antenna). The selection of the spectral cut-off is somewhat arbitrary for power-law surfaces, but the results described below are insensitive to the exact choice of the cutoff.

The surface spectrum for Europa is not well characterized on meter-scale wavelengths (which determine the rough-surface contributions) to kilometer scale wavelengths (which influence geometrical optics contributions). The best available data for the large scale surface characteristics is obtained by using stereo-derived DEM (digital elevation models) obtained by using Galileo imagery (Giese, private communication, 1998). To sample a variety of terrain types, three different sites were chosen among the available data: a region about the Pwyll crater, the Conamara Chaos region, and a region containing the characteristic wedge shapes observed over many fracture regions on the European surface.

The spatial sampling of the available DEM data varies from 300 m spacing (Pwyll), 100 m (Wedges), to 20 m (Conamara Chaos), while the large scale wavelengths range from 30 km (Pwyll) to 3 km (Conamara Chaos region). Because of the difference in sampling, the large scale slope distribution and RMS slope values should depend on the high frequency cut-off if the surfaces are characterized by power-law height spectra characteristic of planetary topography. The observed RMS slopes (5.3° for Pwyll, 8° for Wedges, and 22° for Conamara Chaos) confirm this expectation. An examination of the slope probability density function (pdf) shows that the distribution of slopes is generically characterized by unimodal distributions with large tails, which are not well fit by Gaussian distributions. The tails of the distributions exhibit slopes that could be greater than some angle of repose. The presence of such large slopes may be due to the fact that the regions chosen are geologically young, or to errors in the stereo mapping methods for regions with large slopes.

A detailed spectrum of the surface heights can be obtained only for the Pwyll region, due to data gaps and patch-size restrictions for the other two data sets. The spectrum for the Pwyll region exhibits the expected power-law behavior over scales ranging from 300 m to 30 km. The spectral decay constant for surface cuts is -2.5, corresponding to a spectral decay constant of -3.5 for isotropic surfaces. Extending this spectrum from 300 m to 0 m predicts that the surface RMS height for the unsampled small-scale surface will be on the order of 7m.

The specular, or geometric optics, return can be shown to be proportional to the product of the Fresnel reflection coefficient times the pdf of surface slopes. Using the slope pdf for the Pwyll region, the predicted geometrical optics contribution decreases linearly in dB space from about -10 dB to -20 dB as the incident angle varies from 0° to about 20° . For incident angles greater than 20° , the geometric optics cross section remains roughly constant at about -20 dB for incident angles smaller than 45° . The presence of this plateau region in the cross section is due to the large tails observed in the slope pdf. A conservative estimate of the geometric optics contribution is to assume that very few surface glints are obtained for surface slopes greater than the angle of repose. This produces a geometric cross section which decreases rapidly for incident angles greater than 30° . Since the geometric cross section merely reflects surface glints, it is nearly frequency independent (although a slight dependence due to the selection of the spectral cut-off may be present). The predicted geometrical cross section for the other wedges and Conamara Chaos terranes is qualitatively similar, but with higher contributions at higher incident angles due to the larger RMS slope values observed.

On the other hand, the return due to the small-scale surface component may exhibit frequency dependence since the Bragg cross section varies as the fourth power of the wavelength. The predicted backscatter levels depend sensitively on the RMS surface height for the small-scale surface, which unfortunately are not available from measurements. It can be assumed that the small scale surface exhibits the same spectral decay as the measured large-scale surface, and that the small-scale RMS surface height varies between 1 to 10 m. For small RMS heights (1m), the cross section varies almost linearly in dB from about -10 dB to about -50 dB as the angle of incident varies from 10° to 45° . Frequency variations in the range from 10 MHz to 50 MHz account for cross-section variations of about 10 dB. For larger RMS height (7 m), the predicted cross-section can be as large as -20 to -30 dB for incident angles from 20° to 45° .

Summarizing the surface scattering results for the European radar sounding model, we conclude that for incident angles smaller than 30° , the expected total cross section is dominated by the geometric optics return (-10dB to -20 dB), which is frequency-independent. For incident angles greater than 30° , the cross section can vary between -40 dB to -20 dB depending on the surface characteristics present. This result is attributable to the rugged nature of Europa's terrain and the large slopes that can be encountered for some of its unusual features as well as difficulties in assessing the presence of slopes greater than the angle of repose. Figure 3 shows the strength of the scattered return (given the radar sounder hardware/processing implementation of the following sections). For this figure, the two-scale scattering model of Europa's surface contrasted with a cosine squared scattering function extrapolated from the known scattering of Europa at microwave wavelengths and assuming -10 dB near-nadir losses.

Models of the scattering from any European ice/ocean interface are problematic because the geometry of any presumed interface is uncertain. Extrapolating from observations on Earth, if cracks are present at the interface they will be much larger than those at the ice-vacuum interface, leading potentially to a very rough interface. On the other hand, this interface may be dominated by accretion or ablation processes, leading to an arbitrarily smooth interface at scales larger than a few centimeters. In the absence of significant height variations in the ice/water interface and given the preferred ice and ocean properties of Table 1, the coherent contribution from this interface is at most a few dB of reflection loss. When random height variations in the interface are present, however, theory (Tsang et al., 1985) predicts that this coherent return will be attenuated by a factor of $\exp(-4k^2h^2)$, where k is the electromagnetic wave number, and h is the RMS height of the interface. This factor is strongly dependent on frequency, and can give rise to large drops in the coherent return if the RMS height is not much smaller than the EM wavelength. Lack of knowledge about scattering from the bottom interface does not allow for a prediction of the effect for any selected instrument configuration. We know only that the attenuation of the coherent return will be greater at higher frequencies for the case of significant height variations at this interface. For this reason, the Instrument Definition Team has chosen a sounding frequency of 50 MHz as the best trade-off between increasing Jovian radio frequency noise (with decreasing frequency) and increased scattering from any ice/ocean interface (with increasing frequency). Assuming scattering from a European ice/ocean interface that is the same as that for the ice surface, Figure 3 shows the expected strength of the return from this interface (as a function of total ice thickness) for the 50 MHz radar sounder described in the following sections.

System Performance

Figure 2 shows the calculated two-way absorption versus depth for the three proposed ice formation processes on Europa and Figure 3 shows the modeled strength of the return from an ice/ocean interface for these processes. For both the marine ice and tidal/tectonic processes (i.e., $T_b=270K$), the ability to characterize any ice/ocean interface or internal layering can be inferred directly from these plots. Recalling that a smooth ice/ocean interface would give negligible reflection losses, Figure 2 shows that the total absorption is less than the nominal instrumental dynamic range over the full range of total ice thicknesses estimated for both marine and tidal/tectonic ice formation processes on anti-Jovian Europa. This is also the case for the rougher ice/ocean interface assumed in Figure 3. In addition, Figure 3 shows that the range of total ice thickness soundable on sub-Jovian Europa is reduced by about one-third (to a little over 2 km for marine ice and 6 km for tidal/tectonic ice formation processes) compared with anti-Jovian sounding.

For the “convection” processes of Figure 2, the deeper warm layer is likely to contain brine pockets as the ice temperature will be above the eutectic point of some chloride salts. Because of this, absorption will become very high (similar to the sea ice of the Baltic Sea or even higher; Table 1) and radio waves will be unable to penetrate the convecting ice to any subsurface ocean. If the boundary is reasonably sharp, there will be a radar reflection from it due to the change in dielectric impedance. The magnitude of the reflection will depend on the brine content in the ice

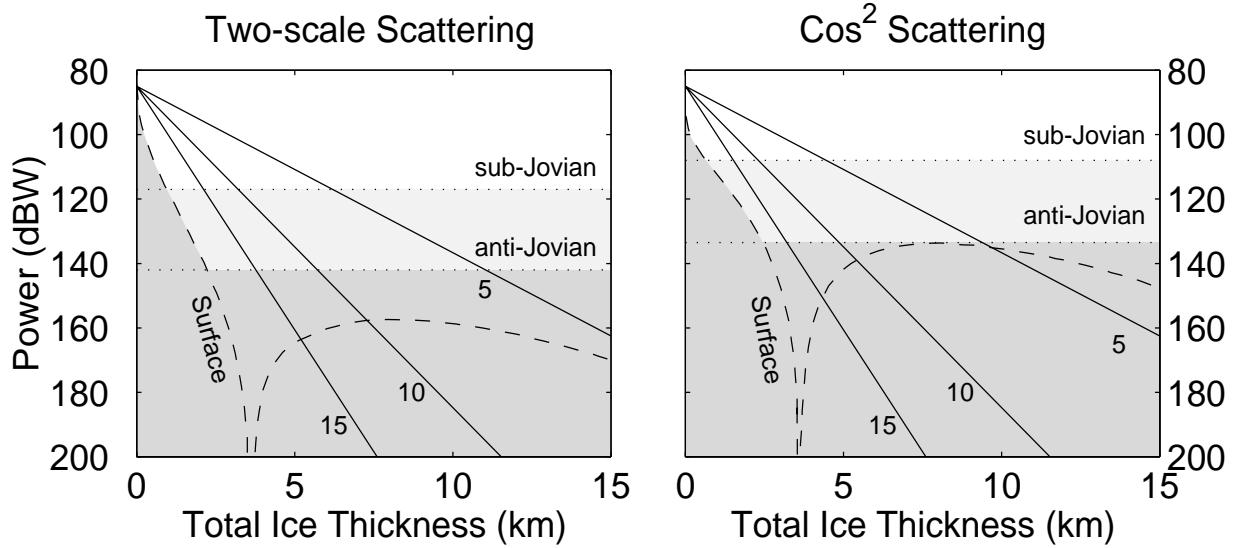


Figure 3. System performance for the recommended 50 MHz Europa radar sounder in the context of two possible scattering models for Europa’s surface (dashed lines). The sub-Jovian and anti-Jovian radio frequency noise limits (dotted lines) are derived from Figure 1 and modified by the processing algorithm appropriate for the surface scattering model. The strength of the return from an ice/ocean interface (assuming the same scattering model as for the surface) over a probable range of Europa ice formation models are presented as solid lines: the line labeled 15 shows the expected ice/ocean return as a function of total ice thickness (i.e., -15 dBW km^{-1}) for the marine-ice model of Figure 2 at equatorial temperatures (see the marine-ice entry for a sulfate-dominated Europa ocean in Table 1); the line labeled 5 shows the expected return again as a function of total ice thickness (i.e., -5 dBW km^{-1}) for an ice/ocean interface given the tidal/tectonic ice formation processes of Figure 2 at polar temperatures (see the dusty (salty) ice entry for 1% lunar soil in Table 1); the solid line labeled 10 (i.e., -10 dBW km^{-1} of total ice thickness) also corresponds to an ice/ocean return for tidal/tectonic processes but at equatorial temperatures and for the dusty (salty) ice entry with 10% lunar soil in Table 1. The darkest gray shading indicates the noise floor for radar sounding on anti-Jovian Europa while the lighter gray shows the much higher noise floor for sub-Jovian radar sounding. Experience with terrestrial radar sounding of ice sheets indicates that laterally continuous returns with a strength equal to the noise floor are routinely detected in radar sounding images. These plots are probably conservative in their estimates of surface noise reduction achievable with the Doppler processing described in Section 4.

and its spatial distribution. A relevant example is the reflection coefficient observed at the boundary between cold-dry and temperate-wet glacier ice with an essentially uniform distribution of water pockets which is typically about -20 dB (Bamber, 1987). Assuming a similar reflection coefficient for convection processes on Europa, Figure 2 shows that it is very likely that the 50 MHz instrument described below will penetrate the full range of expected rigid lid thicknesses and allow characterization of the interface with the convecting layer beneath. Figure 2 also shows that any icy crust formed by a tidal/tectonic process dominated by ocean water injection and rapid freezing could also be characterized by “sea-ice”-like absorption at depths where temperatures are above the eutectic point of any constituent chloride salts. If this were the case it would only be the upper surface of this sea-ice layer that could be characterized.

3. Hardware

This section describes the radar sounder hardware corresponding to the system performance presented in Figure 3. Given the sounding model of Section 2, the sounder implementation described below (when coupled with the processing and sampling strategies described in Sections 4 and 5, respectively) should sample globally the ice crust beneath the major surface features of Europa to depths of up to 20 km. These soundings will have a spatial resolution of one to two km (for orbit elevations of 100 to 200 km) and a depth resolution of ~100 m.

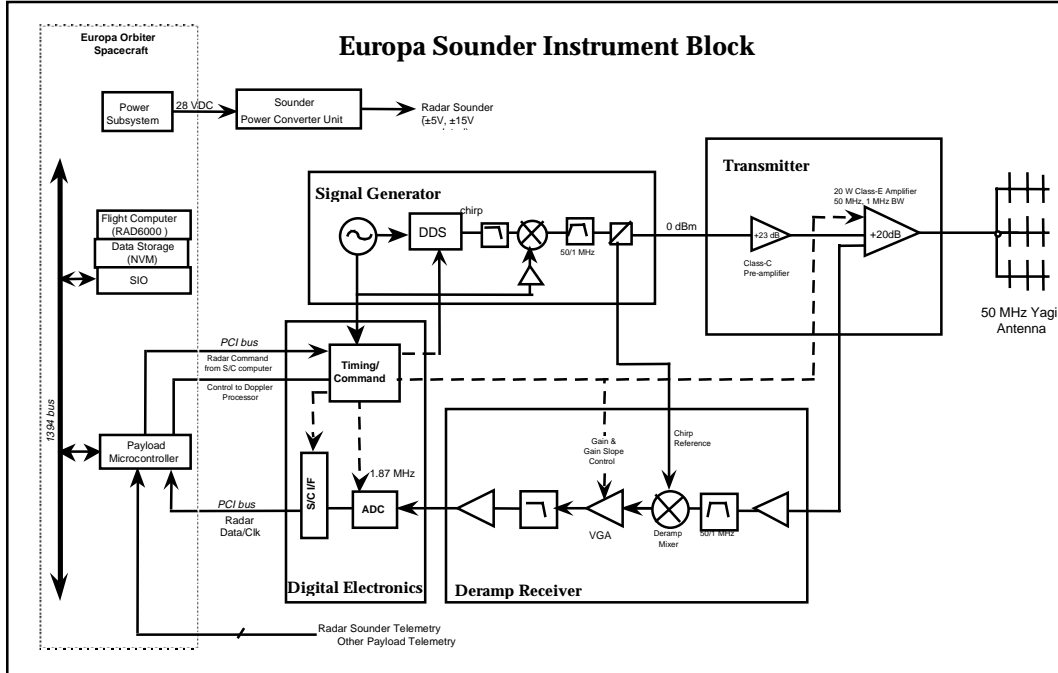


Figure 4. Block diagram of Europa radar sounder.

The hardware consists of a Yagi antenna, a 20 W transmitter, and a sensitive receiver with digital output to the spacecraft computer bus (Figure 4). Data reduction is assisted in the radar hardware by employing a means to reduce the echo dynamic range and a “deramp” mixer to reduce the signal bandwidth necessary for processing. The primary data reduction and science data extraction is performed in the processor by azimuth compression and echo averaging. The spaceflight computer (SFC) controls the radar functions through a series of registers thus reducing the complexity of the radar digital hardware. The radar provides internal timing, critical to a coherent system, with a stable local oscillator (STALO). Other critical timing functions (e.g. the transmit/receive window control) are set by the SFC. The primary operating frequency for the radar system is 50 MHz, which corresponds to a 6 m wavelength in a vacuum and ~3.5 m in ice.

Antenna Characteristics

An array of three standard 3-element Yagi antennas is proposed for this system (Figure 5). This antenna array will form a relatively narrow cross-track beam pattern, have high gain, and have high front-to-back ratio. The antenna elements are assumed to be made of titanium with diameters of 1.5 mm. Titanium is relatively low in conductivity (about 2.5×10^6 mhos/m), but is superb in terms of stiffness and weight, and has been widely used for spaceborne antennas. Figure 6 shows numerical simulations of the 50 MHz antenna pattern in the cross- and along-track planes.

The array has a maximum directivity of approximately 12 dB in the nadir direction with 3-dB beamwidths of about 20° and 100° in the cross- and along-track directions. The first side lobes in the cross-track direction are roughly 37° away from the nadir direction and are about 13 dB down in the gain level. Since the antenna array will be used for both transmitting and receiving, the side lobe levels will be 26 dB below the main lobe. The front-to-back ratio is about 20 dB at 50 MHz. The antenna impedance will be matched to 50Ω through transformers, or through the transmission lines between the RF electronics and the antenna elements' feeding points, as has been done for many other types of antennas. The current design has a natural mechanical frequency of roughly 1 Hz and can withstand an acceleration of about 0.2 G. The total mass for the antenna, including the storage and release hardware, is estimated to be less than 4.7 kg.

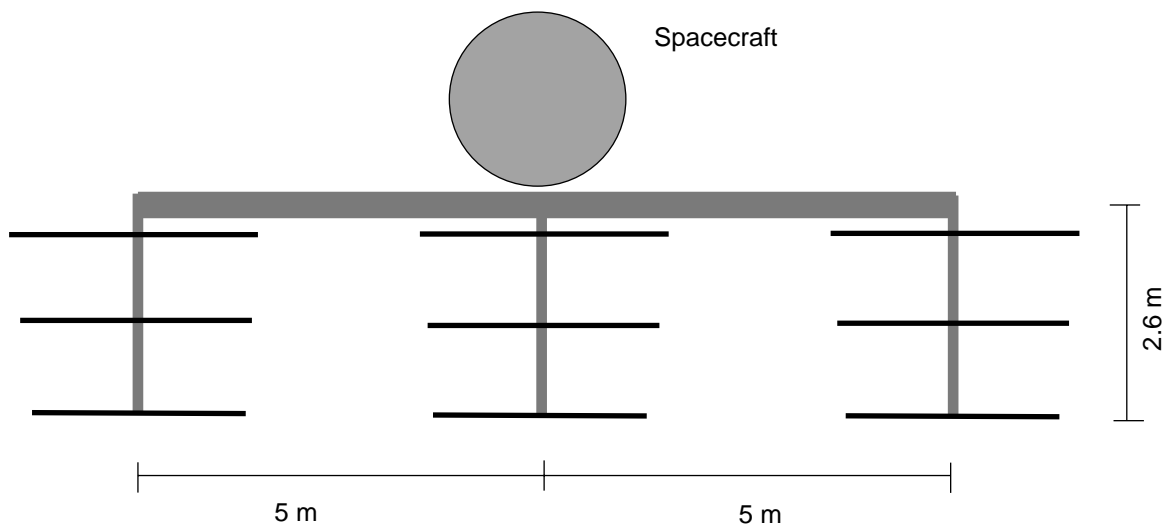


Figure 5. Fully deployed antenna structure. The thin solid lines in the figure represent the antenna elements; and the gray bars represent the supporting booms. The array will be pointed toward Europa with its supporting boom oriented in the cross-track direction.

Large, complex and lightweight antenna arrays have been successfully deployed for various satellites. The Forte satellite launched in 1997 by Los Alamos National Laboratory deployed a 20-element log-periodic-array (LPA) antenna that extends about 11 meters and contains elements as long as about 5 meters. In comparison, the Yagi array for the Europa radar is relatively simple. The light structure is a new concept in antenna design and initial studies, including a review of the mechanical concept, indicates that it is feasible.

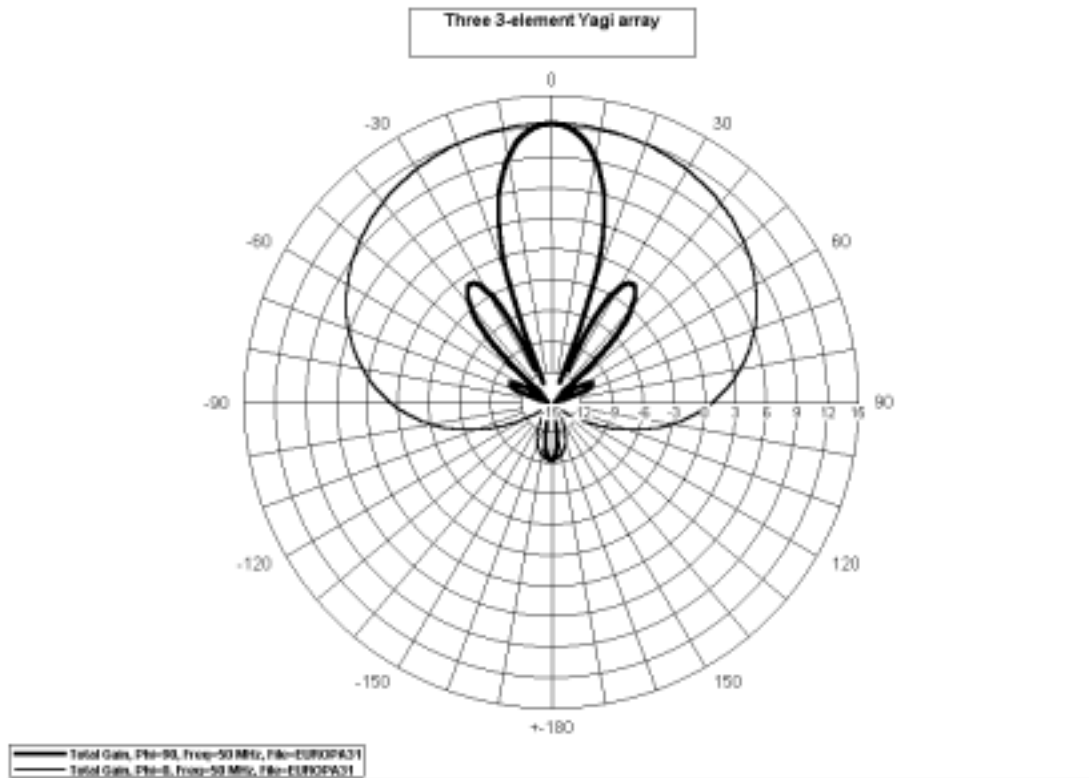


Figure 6. Simulated one-way antenna patterns in the cross- and along-track directions. The 3-dB beamwidth is about 20° in the cross-track direction, and about 100° in the along-track direction.

Signal Generator

The radar transmits a linear-FM (chirp) waveform using direct digital synthesis (DDS) technology, where a numerically controlled oscillator (NCO) is used to derive the frequency modulated sine wave output. Since the frequency and bandwidth requirements are relatively modest, a low power NCO device can be used. Of critical concern, however, is the radiation tolerance of this device, since the expected radiation exposure (within the payload science stack) is on the order of 1 Mrad. One suitable NCO is the Stanford Telecom STEL-1173RH, which is a radiation hardened version of the STEL-1173. It combines low power CMOS technology with an architecture that is power efficient and has a total dose capability of 1 Mrad. The NCO can generate the chirp at baseband that is then upconverted to the 50 MHz transmit frequency using a mixer. This approach, rather than directly generating the chirp at RF, has been selected for lower power consumption which for this device is proportional to clock frequency. In addition, there are other candidate radiation-hardened NCOs available at lower clock rates.

Transmitter

A key element of the Europa Sounder instrument is the high power, very high efficiency transmitter amplifier. This amplifier is currently under development by Caltech and JPL for the Advanced Radar Technology Program (ARTP). Based on currently available performance data of the amplifier breadboard, it is believed that a 20 Watt amplifier, operating at approximately 20% duty cycle, with 0.85 MHz bandwidth, 50 dB of gain and 90% efficiency is achievable using a combination of a Class-A preamplifier and a Class-E power amplifier. In the severe radiation environment of Europa, the current best estimate for amplifier efficiency exceeds 80%. The Class-E amplifier also acts as a T/R switch for further mass reduction. The transmitter amplifier can operate directly off the spacecraft-provided 15V power supply with some additional regulation.

Receiver

The high dynamic range requirement results in the need for dynamic gain control. The deramp design uses the transmit chirp waveform to downconvert the chirp rather than use a conventional local oscillator. This deramp technique will reduce the system data rate by performing analog chirp compression. A variable gain amplifier (VGA) is used to reduce the dynamic range requirement by weighting the deramped chirp. Monolithic microwave integrated circuit (MMIC) technology must be implemented due to the severe mass and power limitations.

Digital Electronics

The digital system consists of a 12-bit analog-to-digital converter with a timing/command circuit and spacecraft interface to be implemented using field programmable gate arrays (FPGA) or an application specific integrated circuit (ASIC). The spaceflight computer (SFC) controls the radar data collection and processes the data after it has been written to spacecraft data storage. The SFC writes parametric commands for the radar hardware by means of the spacecraft input/output (SIO) module. The SIO module interfaces the SFC to the 1394 bus. The commands are received by the payload microcontroller attached to the 1394 bus; this microcontroller interfaces to the radar hardware using a PCI bus. The commands are received by the radar digital electronics through a PCI interface circuit and are used to program the timing/command circuit. This circuit generates the signals used to program the digital signal generator as well as to provide clock, control and timing signals to both the RF and digital electronics. These signals include setting the pulse repetition frequency (PRF), triggering radar transmission, setting the data sampling window and triggering the ADC.

The ADC samples the video signal and converts it to parallel 12-bit digital words. The sampling clock rate is set to 2.2 times the bandwidth (or 1.87 MHz). The ADC will sample roughly 750 μ s of the echo return period resulting in an average data rate of about 6 Mbps to the SFC, producing approximately 1400 samples per transmission at a PRF of 375 Hz. The radar digital electronics packs two 12-bit data words from the ADC into a single 32-bit word and transfers it across the PCI bus to the microcontroller at a rate of approximately 250 kHz. The microcontroller then writes the data into local memory, provides any necessary formatting and sends the radar packets

Europa Radar Sounder Instrument Definition

to the data storage system over the 1394 bus where the SFC performs real-time processing (see Section 4).

System Parameters

Table 2. Europa Sounder system parameters.

Parameter	
Transmit Power ¹	20 W
Antenna Gain	12 dB
Pulsewidth ¹	500 μ sec
PRF	375 Hz
Bandwidth	0.85 MHz
Receiver Dynamic Range w/ VGA	90 dB
A/D Quantization	12-bits/sample

¹ Other combinations may be considered to mitigate any potential sidelobe problems

Mass/Power Estimate

Table 3. Europa Sounder instrument mass and power estimates. These estimates assume a 50% margin in power consumption to compensate for the actual Europa radiation environment and 50% mass margin to allow for additional shielding of critical components. The design does not include any redundancy due to severe limitations on mass and power.

	Size ¹	Mass	Power
Antenna Subsystem		4.7 kg	0.0 W
Yagi	10-meter	4.0	0.0
Cables		0.3	0.0
Mounting Brackets		0.4	0.0
RF Subsystem	4 slices	2.15 kg	12.0 W
Signal Generator	2 slice	0.85	5.0
Transmitter (20W, 80% eff., 18.75% duty)	1 slice	0.80	4.7
Receiver	1 slice	0.5	2.3
Digital Subsystem	3 slices	1.15 kg	3.9 W
ADC	1 slice	0.39	1.6
S/C interface & Timing	2 slices	0.76	2.3
Other Hardware	1 slice	1.0 kg	4.0 W
Power Converter Unit (80% eff.)	1 slice	0.5	4.0
PCI Backplane		0.5	0.0
Total Sounder Instrument	8 slices	9.0 kg	19.9 W

¹A slice is 4"x6" PCI board compatible with science stack

Spacecraft Interface Assumptions

The sounder instrument will be co-located with the other science payloads within the science stack and will therefore share resources including system packaging, shielding, thermal control, and power. The flight computer used for on-board data processing and radar control is also shared with the other science payloads as well as the orbiter avionics. The electrical interface to the spacecraft is via a PCI bus interface to a payload microcontroller. The microcontroller then communicates with the flight computer and data storage over the 1394 high-rate data bus. Power to the Sounder is provided by Power Converter Units (PCUs) within the science stack and shared by other science payloads. Other spacecraft interface assumptions include:

- There will be 1 science stack dedicated to all science payloads. The stack is limited to about 20 "slices" per stack. The sounder instrument requires 8 slices maximum (7 plus 1 reserved for power supply). The slice dimensions are approximately 4" x 6".
- The spacecraft will provide data storage (non-volatile memory with 2.2 Gbits dedicated to all science payloads) and two flight computers (RAD 6000, 30 MIPS or better) for command sequencing and real-time data processing.
- The spacecraft power subsystem includes power control and switching to regulate the main bus power plus a battery for energy storage. The current assessment by the Europa Orbiter avionics group is that the spacecraft can handle the sounder's peak and average power requirements without needing an additional energy storage device. The instrument has a dedicated PCU within the science stack. Present voltage requirements for the sounder instrument are ± 5 V and +15 V.
- The radiation exposure is 4 Mrad behind 100 mil aluminum (inside the spacecraft bus) and lower within the stack. Parts should be selected with 1 Mrad rating, with additional derating shielding to lower exposure to 667 krad.
- The science stack temperature is regulated to 0-40° C.
- Each slice is capable of dissipating 10 W.

4. Processing

This section describes representative science data output capabilities of the Europa Radar Sounder. The baseline mode is expected to return to Earth all data collected by the sounder, processed on-board into waveforms having depth and along-track resolutions equal to the radar's capabilities. A second mode offers waveforms averaged in depth resolution or in along-track spatial resolution, either version having a lower data rate than the baseline mode. The purpose of this mode is to allow survey radar sounding to co-exist with other Europa observations such as geodesy, or to adapt to any other data rate or data volume constraint. Finally, a third mode supports the digitized radar sounder data, prior to on-board waveform processing, captured on a per-pulse basis. This mode, whose data rate and volume would far exceed routine operating

capabilities of the sounder telemetry, requires on-board buffer storage prior to down-link at a slower rate. Data in this mode may be useful for initial validation of the sounder's performance, and for specialized (and relatively rare) observations of selected regions of Europa.

“Waveform” in this discussion is meant to imply a mapping of signal strength as a function of delay time, which in turn is proportional to depth of penetration of the radar's emitted energy into the ice. Once the waveforms are returned to Earth, sequences of them may be combined to form profiles of ice penetration along the sub-satellite tracks. Each waveform is the product of processing the observed echoes of several thousand individual pulses transmitted by the radar. The radar sounder and its on-board processing is designed to: (1) resolve the along-track footprint size of each waveform to be as small as possible (typically < 2 km), (2) resolve the depth measurements of scattering layers and potential ice/water interfaces (typically ~ 100 m), (3) measure the mean altimetric elevation and large-scale roughness of the surface of the ice (estimated accuracies for which are ~ 15 m and ~ 30 m, respectively), and (4) estimate the radiometric properties of reflection and losses within the ice. Spatial (along-track) resolution is taken in this context to mean the size of each individual waveform's footprint after on-board (Doppler) processing, and depth resolution implies the size of each depth data bin.

The science waveforms to be produced by the Europa Sounder may differ from those described in these paragraphs. Implementation details of processing and waveform generation will be determined by the final design of the sounder. The actual waveform telemetry formats will take into account preferences and/or requirements of the science community, subject to constraints that may be imposed by the radar design, on-board processing resources, and the capacity of the data down-link.

The radar sounder, even at the relatively low pulse repetition frequency (PRF) of about 400 Hz suitable for the 50 MHz band when operating from 100 km above the surface, will be turning out approximately 100 times more data than the mission telemetry can accommodate continuously in real time. On-board processing is essential to reduce the data volume to a manageable size. Initially this may be perceived as a limitation by those scientists who are used to having in hand all of the data produced by (airborne) sounding radars, but it is a true and fundamental constraint. Several consequences ensue. There must be some form of data rate reduction implemented in the sounder, between the radar and the science data stream. Even if a snapshot view of a set of individual radar echoes were possible from time to time, routine operation will have to turn out "processed" science data on board.

On-board Processing

Fortunately, typical ice sounding data is characterized by rather extensive redundancies when compared on a pulse-to-pulse basis. This redundancy can be exploited to reduce the output data rate substantially, and at negligible cost in lost science. The notional on-board processor strategy, outlined below, is a blend of conventional coherent and incoherent integration (known as “stacking” in the sounding community), augmented by similar integrations implemented in parallel data paths. Conventional coherent integration selects only those sounding data whose Doppler frequencies (i.e., the change in frequency due to the relative motion between the sounder

and the sounding target) are at or near zero. The extra data paths arise at offset Doppler frequencies (i.e., the frequency change due to the relative motion of the off-nadir targets). The improvement in sounder performance is directly proportional to the number of such parallel Doppler paths incorporated into the processors. The end result of the waveform processing is a single sounding waveform at each resolved along-track position (Raney, 1998).

The transformation of the pulse-to-pulse radar echo data into waveforms suitable for down-link telemetry to Earth is outlined in Figure 7. Following dynamic range compression and analog-to-digital conversion, the average rate of the raw data from the radar sounder is approximately 6 Mbps. These data are captured in the working memory of the coherent Doppler integrator. Subsequent steps operate on blocks of 64 input range lines at a time to generate coherent migration-corrected sounding waveforms in N parallel Doppler bins, (where $1 < N < \sim 25$, subject to processing limitations). These coherent waveforms are detected, registered along-track, and summed, all in the incoherent waveform integrator. The resulting waveforms represent the full resolution sounding measurement capability of the radar. The telemetry format processor serves as the interface between the full-resolution waveforms and the data down-link system, matching the data delivered to the telemetry system to its mode requirements.

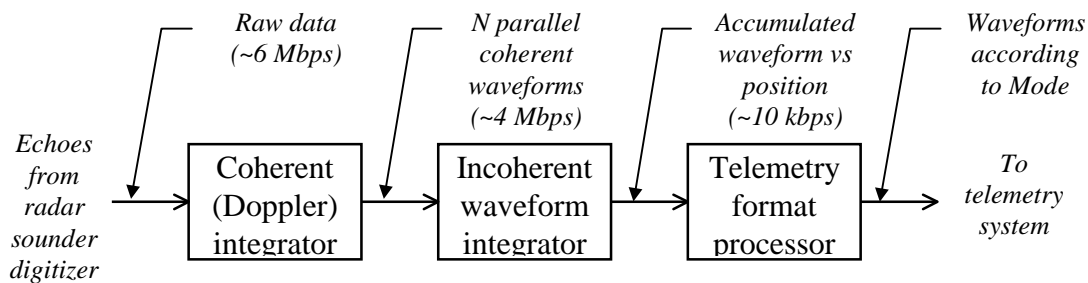


Figure 7. Concept of data flow from the radar sounder to the telemetry system

Requirements

As established by the Europa Orbiter Science Definition Team, the depth resolution is required to be 100 m, or 10% of depth (to 20 km), whichever is larger; the along-track resolution is required to be “at or better than the scale of major surface features” which implies smaller than several kilometers. The across-track resolution is set by inter-orbit distance on the surface, which is likely to be many 10’s of km. There is no explicit requirement on radiometric dynamic range, accuracy, or resolution, although it is implied that all signals of scientific import should be retained in, and recoverable from, the data returned via telemetry. By its very nature, ice sounding data is characterized by very large dynamic range.

Constraints

The baseline Europa Orbiter plan allows a total science data volume of approximately 10^{10} bits for the entire on-orbit mission. The average telemetry data rate allocated to routine science is expected to be about 10 kbps, with 15 kbps to 20 kbps for dedicated purposes. As the data budget must be shared among the entire payload, there is motivation to keep the demand from the radar sounder as low as possible.

The nominal baseline radar sounding mode, denoted here as Mode 1, fits within the mission budget for data volume and data rate. The average Mode 1 data rate of 6.5 kbps is sufficient for continuous telemetry of the full resolution waveforms, and also is low enough that the data volume required by a full set of surface soundings is substantially less than 10% of the mission budget. On the other hand, if there were deeper data rate or volume constraints, then the sounder output data rate would have to be reduced, nominally to 1 kbps, average. This low rate is designated Mode 2, which may be realized either by averaging waveforms in depth (Mode 2.1), or by averaging waveforms along-track (Mode 2.2).

Alternatively, higher rate data may be collected and stored in a buffer, then subsequently down-linked at a lower rate to the Earth. The internal data rate from the radar sounder (prior to the waveform processors) is about 6 Mbps, average. A reasonable lower limit on the useful amount of such data is about 15 seconds, which would be sufficient to allow the mid-beam portion of the antenna illumination to completely scan a given sub-satellite point. This corresponds to about 90 Mb of data. Several such high-rate snapshots could be gathered without overburdening the on-board data storage or down-link resources.

Mode descriptions

Mode 1 and Modes 2 are designed to transmit waveforms at or near the maximum applicable rate, given the constraints imposed by current mission operations. In all modes, the approach is to down-link individual waveforms, each one to include a control word. The (real) waveforms will be represented by floating point magnitudes with one digital number per depth bin. The control word will provide: (1) the surface height (which is proportional to the delay time to the first reflection received at the radar), (2) the amplitude scaling factor, (3) the rate of change of the amplitude scaling factor with depth, (4) the radar PRF (which is a function of satellite height, and on which radiometric and geometric scaling depend), (5) spacecraft time (or an equivalent index of the waveform's along-track location), (6) mode flag, and (7) ancillary data. Note that the amplitude scaling factor and its slope are required in response to the very large dynamic range of reflected power expected for the sounding echoes.

In all modes, data will be included that captures received signal strength both before the first surface reflections, and deeper than the nominal 20 km. The early returns are valuable because: (1) they provide a sample of the prevailing noise, including additive system and ambient environmental noise; (2) they allow an estimate of the presence of sensible range ambiguities; (3) they support estimation of the mean (large-scale) surface roughness, and (4) they serve as a measure of the fine-scale distance between the radar and the surface, thus allowing the sounder to serve as a radar altimeter.

Mode data rates are estimated here without regard to benefits that may be available from data compression schemes. It is reasonable to expect that (lossless) data compression if applied to Modes 1 or 2 could lead to useful benefits. Note, however, that conventional data compression techniques will not work for Mode 3. These data are to first order complex white noise, having no internal redundancies of use to any known data compression algorithm. (Indeed, the optimum "compression" scheme is the default on-board processing.)

Mode 1: Full-Resolution Waveforms (FW).

A notional limit of 6.5 kbps will allow 256 depth bins to be encoded at 20 bits floating point, together with a control word of about 1.4 kb. Thus, a sequence of waveforms in Mode 1 will support generation by an investigator of a profile consisting of soundings each having several hundred degrees of freedom, depth resolution of 100 m over the full 20 km required ice thickness, and spare depth bins to cover early returns prior to the first surface, and late returns to flag deeper responses. This is the default standard operating mode for the sounder.

The satellite's orbital height is the primary determinant of the along-track sounding interval, which will be about 1.4 km for a satellite height of 100 km, expanding to about 1.9 km from a height of 200 km. The statistical degrees of freedom within each waveform, which is proportional to the number of incoherent integrations available, is to first order a constant over this range of orbital heights. Average data rate decreases with increasing orbit height, since one waveform is produced for each resolved along-track sounding interval.

Europa completes one revolution within about 3.5 days. If the radar sounder were to gather data for 7 days at a 50% duty factor, it could generate a complete set of surface soundings, subject of course to the cross-track spacing of adjacent orbits. Such a Mode 1 data set would require less than 2 Gbit.

Mode 2: Averaged Waveforms (AW).

The data rate or volume available to the radar may preclude full resolution sounding for portions of the mission. The averaged waveform modes are designed to meet this contingency, fitting their science return within a 1 kbps limit. Consider one example. If the radar sounder were to gather data in Mode 2 for 7 days at a 50% duty factor, it could provide a survey of the surface, subject to the reduced resolution implied by averaging. Such a survey in Mode 2 would require only about 300 Mbits total data volume. This is much less than the planned on-board storage capacity. Hence, from the data management point of view, a complete Mode 2 sounding data set could be gathered as a background mission coincident with the initial geodesy phase.

Mode 2.1: Averaged Depth Waveforms (AW-D).

One means of reducing the available data rate for each waveform is to aggregate resolution cells that lie at deeper levels, consistent with the depth resolution requirement: the greater of 100 m or 10% of depth. One means of doing this is described in Table 4. In this mode, waveforms would be down-linked that correspond to full resolution along-track, but which have selective depth averaging applied. The amplitude would be encoded as 16-bit floating-point digital numbers at 55 depth stations, leaving about 120 bits available for the control word from an orbital height of 100 km, expanding to several hundred bits for the control word from 200 km height. With such a small control word, it may be necessary in this mode to link control words across a group of waveforms.

Table 4. Mode 2.1 depth bin averaging plan

Depth interval (km)	Number	@Resolution (m)
Pre-surface	5	170*
0 - 2	20	100
2 - 5	12	250
5 - 9	8	500
9 - 13	4	1000
13 - 19	4	1500
19 - 21	2	2000

*The in-ice design resolution of 100 meters expands to about 170 meters in free space.

Mode 2.2: Averaged Surface Waveforms (AW-S).

An alternative means of reducing the available data rate for each individual waveform is to retain full depth resolution, but to aggregate adjacent waveforms along-track, sufficient to meet the governing average data rate of 1 kbps. One means of doing this is to sum several sequential full-resolution waveforms, and to down-link the result at reduced dynamic range. In this mode, from an orbital height of 100 km the averaged surface waveforms would have along-track resolution of about 5.6 km, and they would retain 100 m resolution at all depths. The amplitude would be encoded as 16-bit floating-point digital numbers at 220 depth stations, leaving about 480 bits available for the control word. The corresponding mode from 200 km height would need to average only three waveforms along-track to accomplish virtually the same performance: 5.7 km along-track resolution, 100 m depth resolution, and 16-bit floating-point radiometric resolution, with about 500 bits available for the control word.

Mode 3: Radar Sounder Data Record (RDR).

The average data rate of the radar sounder after the analog-to-digital conversion is on the order of 6 Mbps. As introduced above, these data could be captured directly and placed in memory, there to await an opportunity to down-link the lot at a slower rate. This mode should be regarded as a special case, to be used only when fully justified. Mode 3 can operate in parallel with Mode 1 or with one of the Mode 2 options. Thus, the way is open to record sets of Mode 3 data in parallel with routine surveys. These data could be used as scheduled periodic adjuncts to survey data, or could be focused on selected sites for potential enhancements to the science eventually to be derived from the data.

5. Sampling Strategy

Approximately 10^{10} bits can be telemetered to Earth during the course of Europa Orbiter's nominal mission, and much of this down-link will be devoted to optical imaging and other experiments. Europa can be completely mapped using Mode 1 data collection (i.e., at full resolution) by a radar sounding system with approximately 2×10^9 bits. This could be achieved in 2.5 weeks of operation with a 25% duty cycle. The ability of the radar to function on the night

side of the satellite adds flexibility to its operation and allows mapping to be conducted with the available spacecraft power resources and processing capability.

Two other types of data products in addition to this primary sounding data are deemed desirable by the Instrument Definition Team. First, samples of the unprocessed data (i.e., Mode 3) should be acquired to characterize the permittivity of the European subsurface as a function of depth and to tune the operation of the instrument early in the mission. Down-link constraints dictate that only a few such samples can be acquired. At a minimum, equatorial and polar regions of Europa should both be studied and efforts made to examine the major geologic terrain types on the satellite such as ridged plains, chaotic terrain and impact structures.

Second, global mapping at reduced resolution (i.e., Mode 2) should be undertaken. Sounding data at one-tenth resolution could be acquired over extended periods and stored on board the spacecraft for later telemetry. We note that the radar can serve as a coarse altimeter, providing positional information to augment the geodetic experiments. The total data volume generated by these activities amounts to no more than a quarter of the primary full resolution mapping data set, but greatly enhances the scientific return from the investigation.

6. Other Applications of the Radar Sounder

The primary purpose of the radar investigation is to characterize the three dimensional distribution of ice/liquid and other significant geophysical interfaces beneath Europa's surface. The design of the instrument and data processing should be optimized to that effect. However, a well-designed investigation can also provide information to help address a number of other important issues:

- **Altimetry:** Timing of the first radar return from the surface could be used to augment data from an onboard laser ranger designed to detect the tidal fluctuations predicted for the case of a subsurface sea.
- **Surface Roughness:** Information about the distribution of surface slopes is intrinsic in the clutter recorded by the radar. Steep slopes beyond the angle of repose indicate gravitationally unstable areas of Europa, potentially regions of recent activity.
- **Composition:** The inferred conductivity of Europa's subsurface and its variation with depth could provide a definitive test for the presence or absence of brines.
- **Subsurface Morphology:** The nature and origin of many of Europa's surface features remain uncertain. Geophysical models for feature formation and the subsurface structure can be directly tested by sounding Europa's icy interior.

References

- Bamber, J.L., Internal reflecting horizons in Spitzbergen glaciers, *Ann. Glaciol.*, 9, 5-10, 1987.
- Chyba, C.F., S.J. Ostro and B.C. Edwards, Radar detectability of a subsurface ocean on Europa, *Icarus*, 134, 292-302, 1998
- Corr, H.F. J.C. Moore and K.W. Nicholls, Radar absorption due to impurities in Antarctic ice, *Geophys. Res. Letts.*, 20, 1071-1074, 1993.
- Evans, S., Dielectric properties of ice and snow - a review, *J. Glaciol.*, 5, 773-792, 1965.
- Fanale, F.P., T.V. Johnson and D.L. Matson, Io's surface and the histories of the Galilean satellites, in *Planetary Satellites* J. Burns (ed.) Univ. of Arizona Press, Tucson, AZ, pp. 379-405, 1977.
- Glen, J.W. and J.G. Paren, The electrical properties of snow and ice, *J. Glaciol.*, 15, 15-37, 1975.
- Gross, G.W, I. Cox Hayslip and R.N. Hoy, Electrical conductivity and relaxation in ice crystals with known impurity content, *J. Glaciol.*, 21, 143-159, 1978.
- Gross, G.W., P.M. Wong, and K. Humes, Concentration dependent solute redistribution at the ice-water phase boundary, III, Spontaneous convection: Chloride solutions, *J. Chem. Phys.*, 67, 5264-5274, 1977.
- Kargel, J.S., Brine volcanism and the interior structures of asteroids and icy satellites, *Icarus*, 94, 368-390, 1991.
- McCord, T.B. et al., Salts on Europa's surface detected by Galileo's near infrared mapping spectrometer, *Science*, 280, 1242-1245, 1998.
- McKinnon, W.B, Convective instability in Europa's floating ice shell, submitted to *Geophys. Res. Letts.*
- Moore, J.C. and S. Fujita., Dielectric properties of ice containing acid and salt impurities at microwave and LF frequencies. *J. Geophys. Res.*, 98, 9769-9780, 1993.
- Moore, J.C., A.P. Reid, and J. Kipfstuhl, Microphysical and electrical properties of marine ice and its relationship to meteoric and sea ice. *J. Geophys. Res* 99, 5171-5180, 1994.
- Moore, J.C., J.G. Paren. and H. Oerter, Sea salt dependent electrical conduction in polar ice. *J. Geophys. Res.*, 97, 19803-19812, 1992.
- Ostro, S.J., D.B. Campbell, R.A. Simpson, R.S. Hudson, J.F. Chandler, et al., Europa, Ganymede, and Callisto - new radar results from Arecibo and Goldstone, *J. Geo. Res. Pla.* v97 (e11), pp. 18227-18244, 1992.
- Pappalardo, R.T, et al., Geological evidence for solid-state convection in Europa's ice shell, *Nature*, 391, 365-368, 1998.
- Pappalardo, R.T, et al., Does Europa have a subsurface ocean? Evaluation of the geological evidence., submitted to *J. Geophys. Res.*
- Peters, K.J., Coherent-backscatter effect - a vector formulation accounting for polarization and absorption effects and small or large scatterers, *Phys Rev B*, 46, 801-812, 1992.

Europa Radar Sounder Instrument Definition

- Raney, R.K. The delay/doppler radar altimeter, *IEEE Trans. Geosc. Rem. Sens.*, 36(5), 1578-1588, 1998.
- Tsang, L., J.A. Kong, R.T. Shin, *Theory of Microwave Remote Sensing*, Wiley-Interscience, New York, 1985.
- Weeks, W.F., A.J. Gow, P. Kosloff and S. Digby-Argus, The internal structure, composition and properties of brackish ice from the Bay of Bothnia. - In: *Sea ice properties and processes*, S.F. Ackley and W.F. Weeks (eds), CRREL Monograph. 90-1, 5-15, 1990.